ELSEVIER

Marine and Petroleum Geology, Vol. 14, No. 7/8, pp. 763–771, 1997

Printed in Great Britain
PII: S0264-8172(97)00053-6
0264-8172/97 $17.00+0.00

On the asymmetry of turtle-back growth anticlines

T. Mauduit,* V. Gaullier and J. P. Brun
Géosciences Rennes, UPR 4661 CNRS, Campus de Beaulieu 35042 Rennes

G. Guerin
ELF-Norge, Stavanger, Norway

Received 11 December 1996; revised 30 August 1997; accepted 4 October 1997

Turtle-back anticlines are common structures that develop between facing listric growth faults rooted in a flat lying décollement. Seismic examples from the South Atlantic margins show that whereas their external shape can by symmetric, their internal structure is more generally asymmetric. Laboratory experiments on layered sand silicone models designed to study gravity gliding are used to examine the mode of development of turtle-back anticlines. The results provide information on the ways turtle-back asymmetry develops. The comparison between nature and experiments leads to the following conclusions. The fact that turtle-back anticlines often start symmetric and progressively become asymmetric is due to an increase in coupling between overlying brittle sediments and ductile (salt) layers. The increase in coupling is also responsible for the transition in time and space from dominant seaward faulting to landward faulting for the turtle-back anticlines which never pass through a symmetric stage. The salt diapirs, which separate blocks of the sedimentary cover rafted above the basal décollement at early stages of gravity gliding can play a significant role in the development of turtle-back anticlines. As suggested by previous authors, the diapirs first rise and then fall. Our experiments confirm that diapir fall favours the wrapping of rafted blocks by synkinematic layers. © 1998 Elsevier Science Ltd. All rights reserved

Keywords: Scale modelling ; Gulf of Guinea ; passive margin ; turtle-back structures

Introduction

In deltas or passive margins, the gravity gliding of sedimentary cover above a décollement of weak rocks leads to thin-skinned extensional systems (Vendeville and Jackson, 1992a,b) with a large variety of growth structures. The most common are listric growth faults with associated rollover anticlines. In extensional systems on passive margins, the sense of displacement of the sedimentary cover, the so-called "rafting" of Burollet (1975) and Duval *et al.* (1992), is usually toward the ocean. Intriguingly listric growth faults can be either seaward or landward (e.g. Szatmari *et al.*, 1996; Liro and Coen, 1995) the latter being in kinematic opposition with the sense of displacement at the scale of the whole extensional system. When seaward and landward faults are close to each other an mutually facing turtle-back anticlines are produced. From a geometrical point of view, turtle-back anticline is a double rollover structure with a mirror symmetry plane. As noted by Duval *et al.* (1992) and Lundin (1992), however, although the external structure of turtle-back anticlines is commonly roughly symmetric, their internal structure is generally asymmetric. That indicates a non-synchronous behaviour of the bounding listric faults.

We describe some natural examples of turtle-back anticlines with various degrees of asymmetry. Laboratory experiments on analogue models are used to study the progressive development of turtle-back anticlines and of their asymmetry. The role of the coupling between brittle and ductile layers and that of diapirism on the development of asymmetric turtle-back anticline is discussed.

Natural examples

In a very simplified manner, the structural history of the South Atlantic margins starts with a rifting event during the Late Jurassic to Early Cretaceous, followed by the deposition of a post-rift marine sequence with an Aptian salt layer at its base. The post-rift sequence is affected on both margins by gravitational gliding above the Aptian evaporites, which act as a regional scale décollement. The various structures which results from gravitational gliding and rafting of blocks above Aptian salt, were previously described along the West African passive margin (Jackson and Cramez, 1989; Teisserenc and Villemin, 1989; Duval *et al.*, 1992; Lundin, 1992; Liro and Coen, 1995; Spathopoulos, 1995), and along the Brazil margin

*Author to whom all correspondence should be addressed. Present address: Shell International, EPT-SG Volmerlaan 8, P.O. Box 60, 2280 AB Rijswijk, The Netherlands.

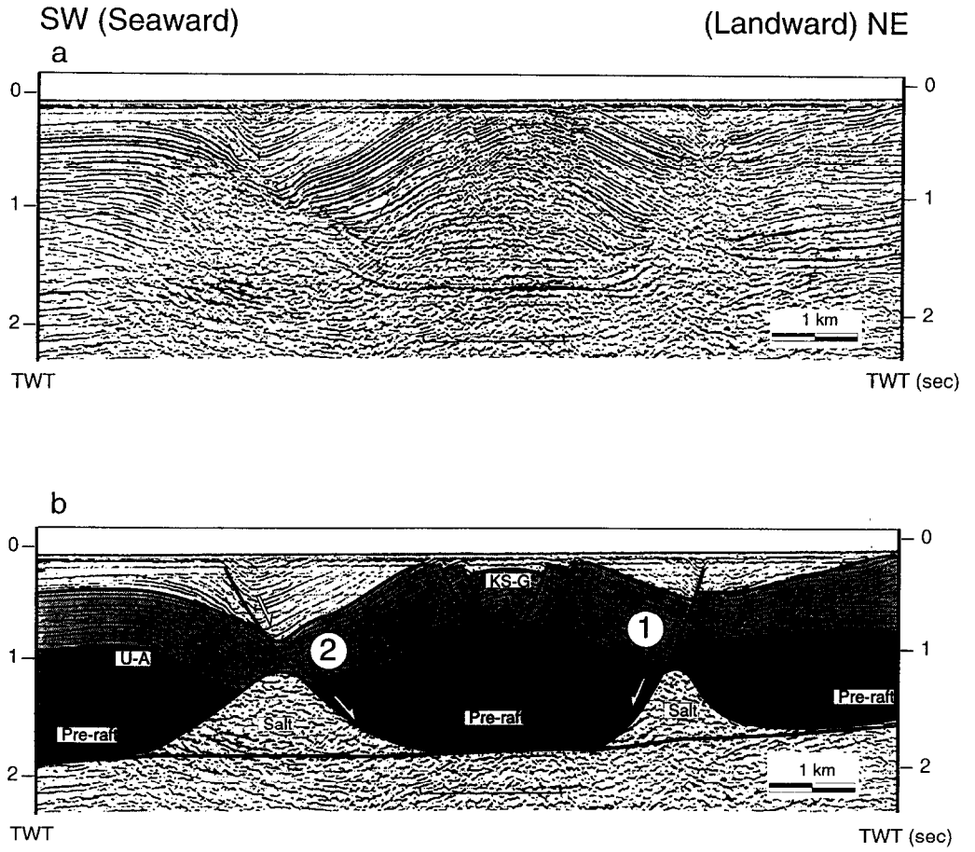

Figure 1 (a) Uninterpreted and (b) interpreted version of a seismic profile showing a turtle-back anticline from the Gabonese margin (KS-G: Keystone Graben; UA = Upper Albian)

(Cobbold and Szatmari, 1991; Demercian *et al.*, 1993; Mohriak *et al.*, 1995; Cobbold *et al.*, 1995; Szatmari *et al.*, 1996).

The seismic profile presented in *Figure 1*, shows a roughly symmetrical 10 km wide Tertiary turtle anticline from the Gabonese margin with a central keystone graben. During the first stages of deformation, rotation on the two boundary faults of the pre-raft series is roughly synchronous. Later evolution displays diachronous fault activity, with a landward-expanding growth sequence. A late regional uplift and associated erosion are superimposed; but the earlier extensional structures are not very modified. This apparently simple example, showing a roughly symmetrical turtle-back anticline, illustrates the complex kinematic evolution of these structures. Moreover, the earliest deposits already show thickness variations, at very early stages of rafting.

The profile presented on *Figure 2* illustrates a 10 km wide symmetrical turtle-back anticline from the Kwanza basin (Angola) which developed from Oligocene to Miocene times. It separates two rafts constituted by the Upper Cretaceous sequence. Though the external shape is roughly symmetric with keystone grabens on both sides, the internal shape is obviously asymmetric. The two listric growth faults appear to have initiated synchronously, but the right hand fault was moving faster as attested by the wedging of the two first layers. Then the two faults have apparently accommodated synchronous deformation up to layer 5 before displacement was entirely localised on the left hand fault.

The section presented in *Figure 3* modified after Demercian *et al.* (1993), shows a 25 km-wide Upper Cretaceous turtle-back anticline coming from the deep offshore of the Campos Basin (Brazil). During the deposition of Cretaceous sequences, displacement occurred only on the seaward listric fault with the deposition of a thick sedimentary wedge. This fault corresponds today to the present upslope limits of the pre-raft series. After the deposition of the last Upper Cretaceous sequence (5 on *Figure 3*), a landward fault started to develop along the upslope flank of a salt diapir which controlled the deposition of the early Tertiary. This evolution is here entirely diachronous.

Modelling principles and techniques

The experiments simulate extension due to the downslope gravitational gliding of sediments with prograding depositional sequences. The modelling techniques are similar to those conventionally used for experiments on brittle-ductile systems at the Laboratory of Experimental Tectonics of the Géosciences Department, Rennes University. Brittle sedimentary cover is represented by sand with a mean friction coefficient Φ of 0.58. Salt has a ductile behaviour which is represented by Newtonian silicone putty with a viscosity μ of 9×10^3 Pas and a density of 1.2 g/cm^3 at 30 C (see Nalpas and Brun, 1993, Appendix 1).

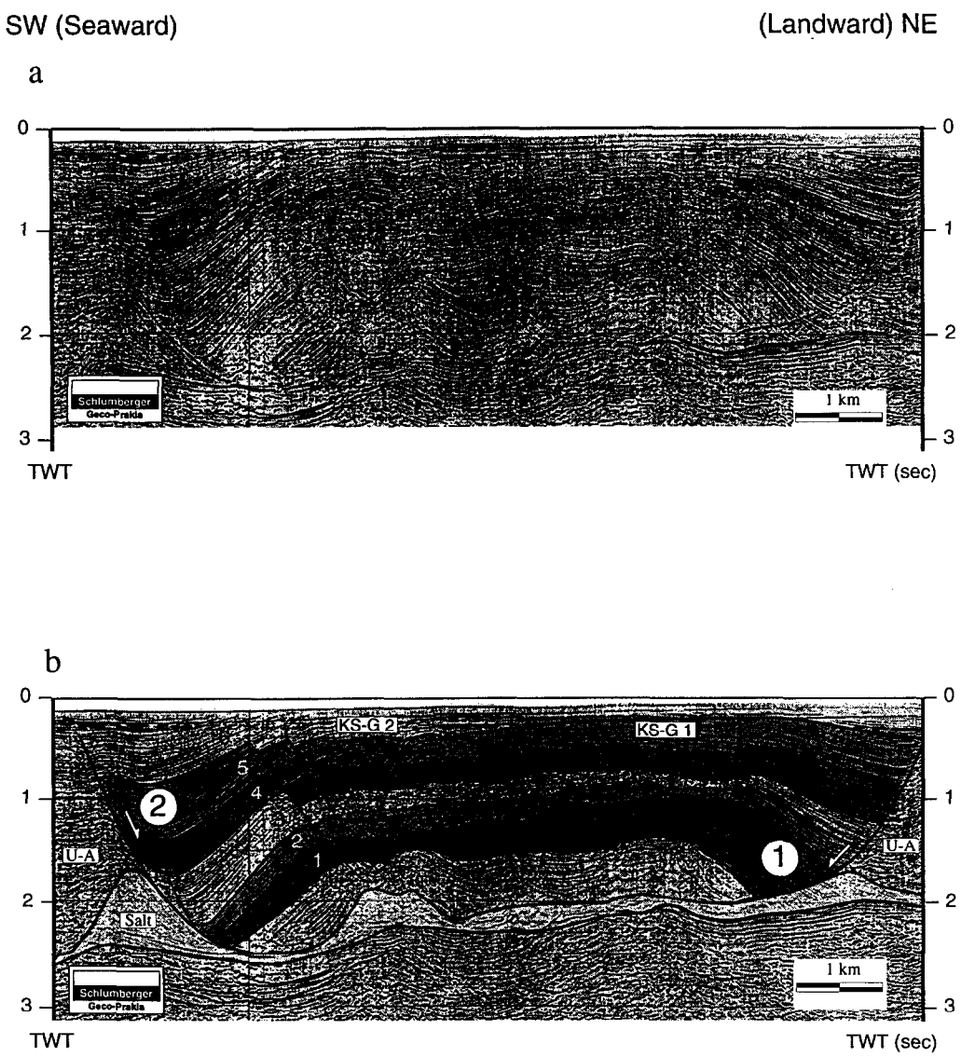

Figure 2 (a) Uninterpreted and (b) interpreted version of a seismic profile showing a turtle-back anticline from the Kwanza Basin, Angola (KS-G 1 and 2: Keystone Graben). The seismic section comes from a non exclusive proprietary survey owned by Geco-Prakla (U.K. Limited). Permission to use these data is gratefully acknowledged. (KS-G: Keystone Graben; UA = Upper Albian)

The linear dimensions of models are scaled down by a factor of 10^5 (1 cm representing 1 km), with a density ratio equal to 1, i.e. densities equivalent in models and rocks. The stress ratio is equal to 10^5. For a viscosity of natural salt of the order of 10^{18} Pas (Van Keken *et al.*, 1993), viscosities are scaled down by a factor of 10^{14}, strain rates by a factor of 10^9 and time by 10^9 (1 h represents about 10^5 years).

Models were built in a 50 cm × 100 cm box, with a rigid removable endwall and a planar rigid base, and consisted of a 1 cm thick silicone layer to represent the décollement layer overlain by a sand overburden to represent the sedimentary rocks. The brittle overburden is composed of prekinematic layer which corresponds to sediments deposed over the basal silicone layer before the onset of extension. The box is then inclined with a basal slope angle constantly at 2° and the down-slope endwall of the box is removed to allow free gliding. Successive syn-kinematic sand layers of alternating colours are then deposed at regular time intervals [12 h for model 1 (*Figure 4*), 1 h 30 for model 2 (*Figure 6*), and 1 h for model 3 (*Figures 6 and 7*)]. Each new deposit simulates a progradation with simultaneous aggradation above the previous deposits. Top views were photographed at regular time intervals, before deposition of each new layer. The experiments are performed at a temperature of 30°C allowing a better control of silicone viscosity and shorter durations of experiments.

Experimental results

Wrapping of horizontal rafts

Figure 4a shows the final section of an experimental model where the prekinematic cover and ductile layer had opposite wedge shapes. Sedimentation was achieved by steps of 4 mm every 12 h. The section displays four rafted blocks of the prekinematic layer separated by diapirs whose width and height increase downslope. Syn-kinematic layers are wrapped around the prekinematic blocks. *Figures 4b–e* present a layer-to-layer restoration

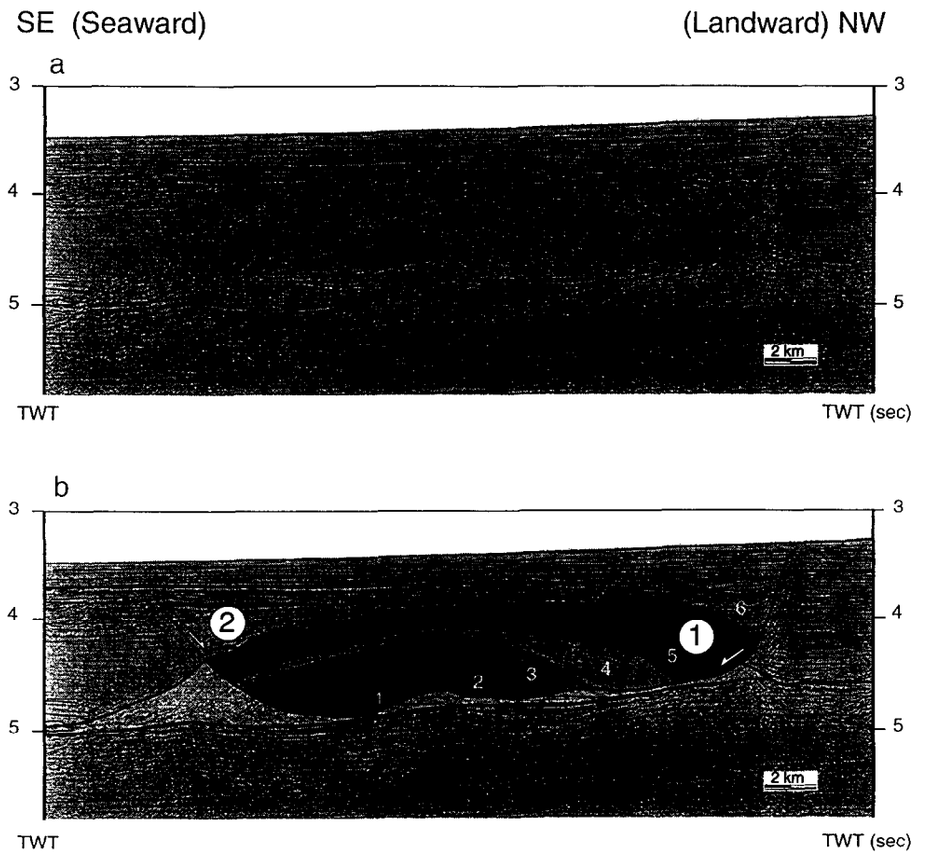

Figure 3 (a) Uninterpreted and (b) interpreted version of a seismic profile showing a turtle-back anticline from the Campos Basin, Brazil (modified after Demercian *et al.*, 1993). (1 and 2: chronology of faulting)

using the final section and top views taken before each new layer deposit. *Figure 4e* presents the end of diapir rising between the rafted blocks before the first layer deposition. Note that the diapir width increases downslope from the very early stages of deformation. During later stages (*Figure 4d–b*), the deformation of synkinematic layers shows that the amplitude of diapirs tends to decrease as their width increases. In other terms, the diapirs fall (Vendeville and Jackson, 1992b). The upslope diapir has the smallest amplitude and the sedimentary depo-centre seated on its top is the thickest. Faults that accommodate diapir fall start first upslope (*Figure 4c*) and develop later downslope (*Figure 4d*). These observations indicate that diapir fall is faster upslope than downslope. This is in agreement with the dynamics of gravity gliding (Brun and Merle, 1985; Merle, 1986) which involves a component of vertical thinning stronger in the upslope domain of gliding slabs than in the downslope domain. The wrapping of the prekinematic layer blocks by synkinematic layers demonstrated by this experiment is one of the basic processes associated with turtle-back anticlines.

Bending of prekinematic rafts

Figure 5a shows an example of a turtle-back anticline constructed around a central raft which has undergone a progressive bending during deformation and sedimentation. Sedimentation was achieved by steps of 4 mm every 1 h 30. The total amount of sedimentation reaches three times the thickness of the prekinematic layer. Extension was strong enough for the base of the sand layer to come into contact with the box basement. As a consequence, the silicone is present within rollers on each side of the turtle-back anticline and below its arched base. The layer-to-layer restoration of *Figure 5b–f* shows the progressive development of the structure.

The turtle-back anticline has a nearly symmetrical external shape. The bending of layers is accommodated by a symmetrical system of conjugate normal faults defining a central graben. Such a graben is called by many authors keystone graben (e.g. McClay and Ellis, 1987; Vendeville and Jackson, 1992b). This fault system starts to develop at an early stage and had remained active throughout the experiment (*Figure 5b d*).

At the earliest stage (*Figure 5f*) the central raft is bounded by two emerging diapirs on which the first layer is deposited. Then the layer is stretched, allowing the diapir to emerge again and a new layer is deposited (*Figure 5e*). During the following steps of layer deposition, the earlier layers are rotated downward on both limbs of the diapirs (*Figure 5d–b*). As in the previous experiment, the amplitude of the diapirs is lower upslope than downslope indicating a fall starting after the deposition of the layer 3 (*Figure 5d*). Diapir fall is accompanied by the development of a seaward listric fault at diapir top, the turtle-back anticline has developed almost symmetrically until stage (d) when the process became asymmetric.

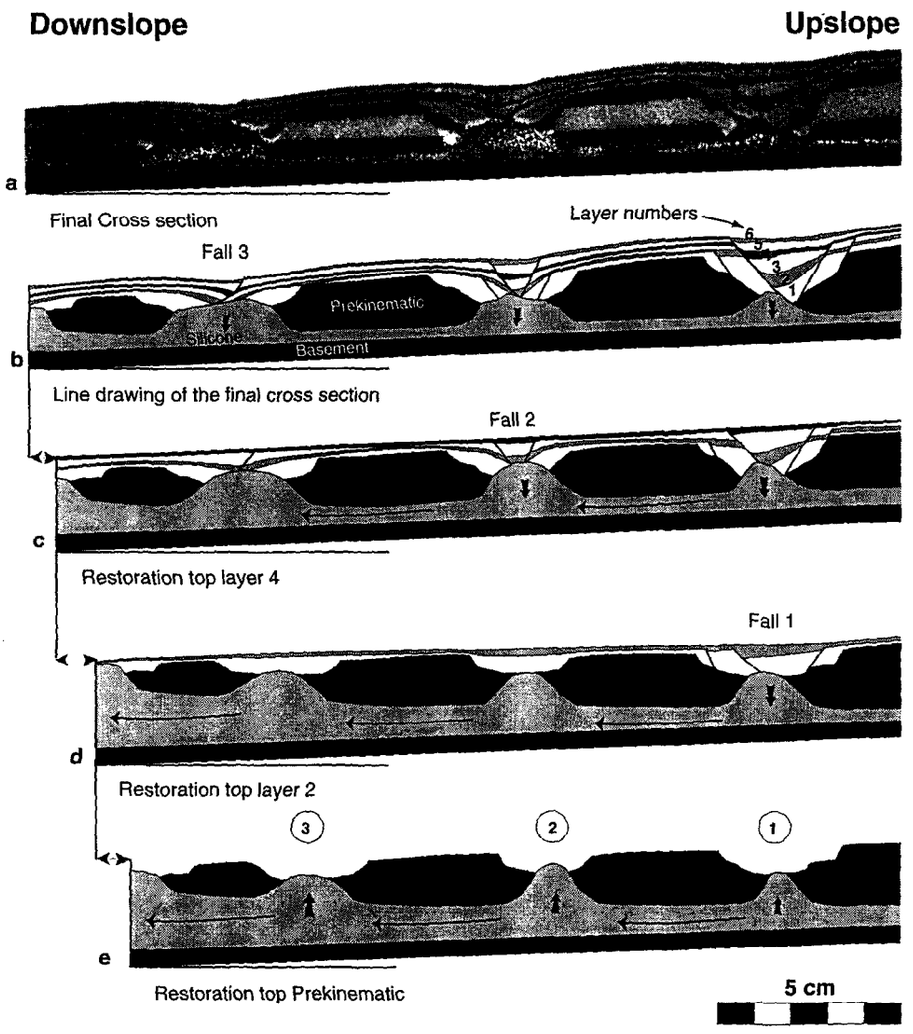

Figure 4 (a) Model cross section of a turtle-back anticline obtained with a low sedimentation rate. (b–e) layer to layer palinspastic restoration of this section

Diachronism of facing listric faults

The two previous experimental models exemplify the role of early diapirs and their rise and fall dynamics on the development of turtle-back anticlines. *Figures 6* and *7* present an example of a turtle-back anticline which developed in a totally different way. Sedimentation was achieved by steps of 4 mm every hour.

The sequence of top views (*Figure 6*) shows the development of a seaward listric growth fault labelled 1 on photographs. This fault was extremely active from layer 4 (*Figure 6a*) to layer 7 (*Figure 6d*). Its activity then strongly decreased (*Figure 6e* and *f*) to finally stop (*Figure 6g*). A second listric growth fault labelled 2 on photographs is landward and facing the previous one. This fault started slowly during deposition of layer 5 and layer 6 (*Figure 6b* and *c*) to become strongly active at later stages (*Figure 6d–h*). Both faults were not initiated at the same time and therefore are partially diachronous. Moreover during their common lifetime they were active at different displacement rates. The seaward fault dominated in the first part of the deformation history and the landward during the later part. The transition is clearly seen on *Figure 6d* and *e*.

The resulting structure (*Figure 7a* and *b*) is an asymmetric turtle-back anticline. The restoration of early stages (*Figure 7g* and *h*) together with corresponding top views (*Figure 6a* and *b*) suggest that the landward fault could be due to the bending of the seaward fault hangingwall. During rapid displacement along the seaward fault, a graben accommodated the bending of the hanging wall. When displacement rate along the seaward listric fault started to decrease, the landward fault of the graben became the landward listric fault 2.

Discussion and Conclusion

Asymmetry of turtle-back anticlines

Seismic sections (*Figures 1* and *2*) show examples of turtle-back structures that initiate around a raft made of prekinematic layers and bounded by salt diapirs. In *Figure 1*, both faults were acting at almost the same rate during the deformation-sedimentation history. It is only at a later stage that the rate of displacement became faster on the landward fault. In *Figure 2* both faults were acting at the same time but the seaward fault dominated at an early stage (layer 1) and the landward fault at a later

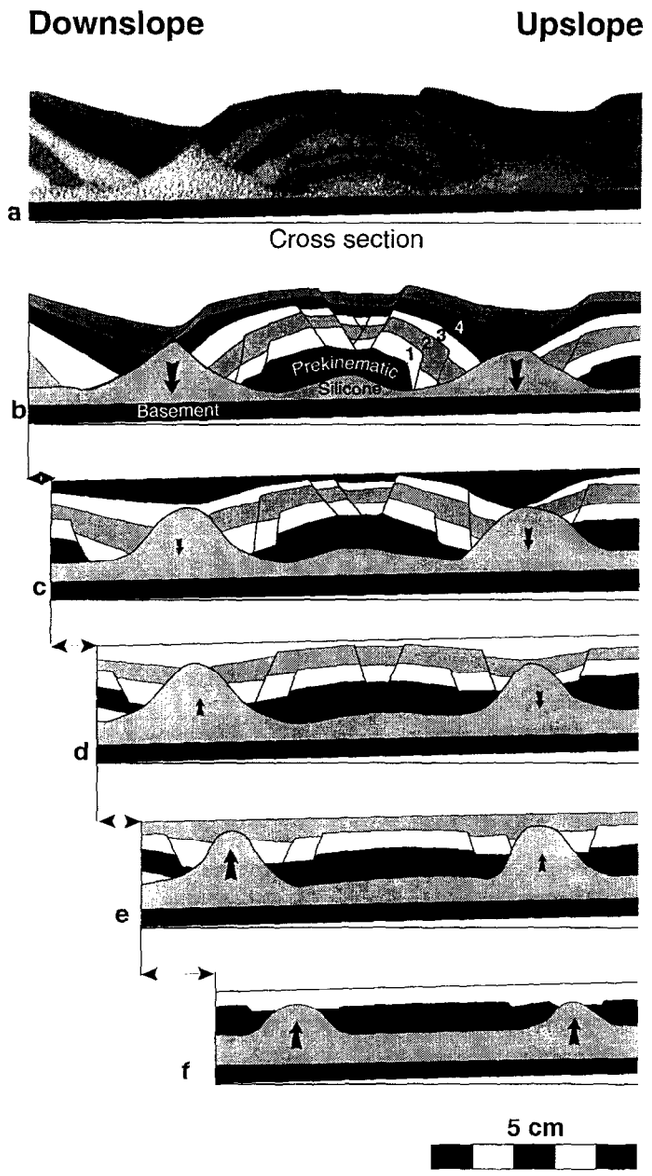

Figure 5 (a) Model cross section of a turtle-back anticline obtained with a medium sedimentation rate. (b–f) layer to layer palinspastic restoration

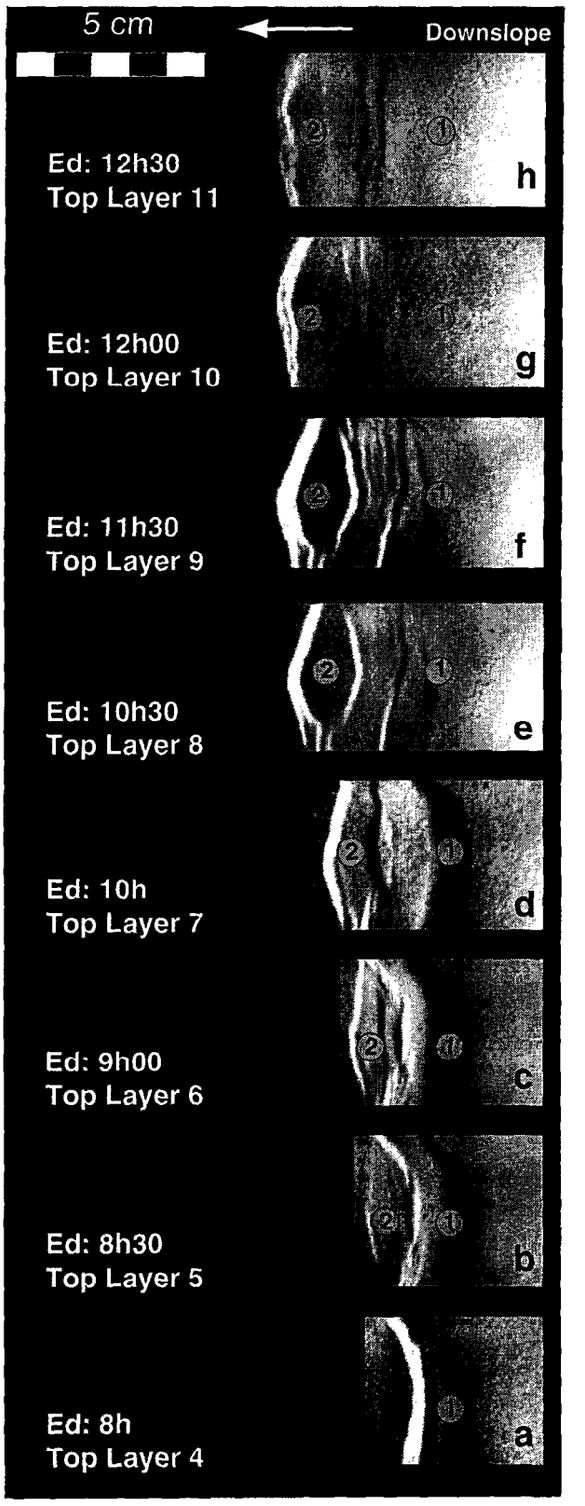

Figure 6 Sequential top views of a model with a high sedimentation rate showing the diachronous development of two facing listric faults seaward (labelled 1) and landward (labelled 2). Illumination from the right

stage. These two examples illustrate the fact that turtle-back anticlines could result from various types of interaction between two facing listric growth faults. Other examples (Duval *et al.*, 1992; Worrall and Snelson, 1989; Lundin, 1992) support this conclusion, and in addition to the examples described here, show that turtle-back anticlines are more generally asymmetric.

Transition in time from symmetry to asymmetry

Both seismic lines and experiments exemplify that during synchronous deformation and sedimentation, a transition often occurs from symmetrical to asymmetrical structural and kinematic settings. The sand-silicone models help understand the mechanical reason for this. Silicone putties in experiments, or salt in nature, are ductile materials which couple or decouple the sedimentary cover to or from the basement. For a constant displacement rate of the gliding slab, the mean shear strain rate in the ductile layer is inversely proportional to the thickness of the brittle layer. Because the strength of the ductile layer

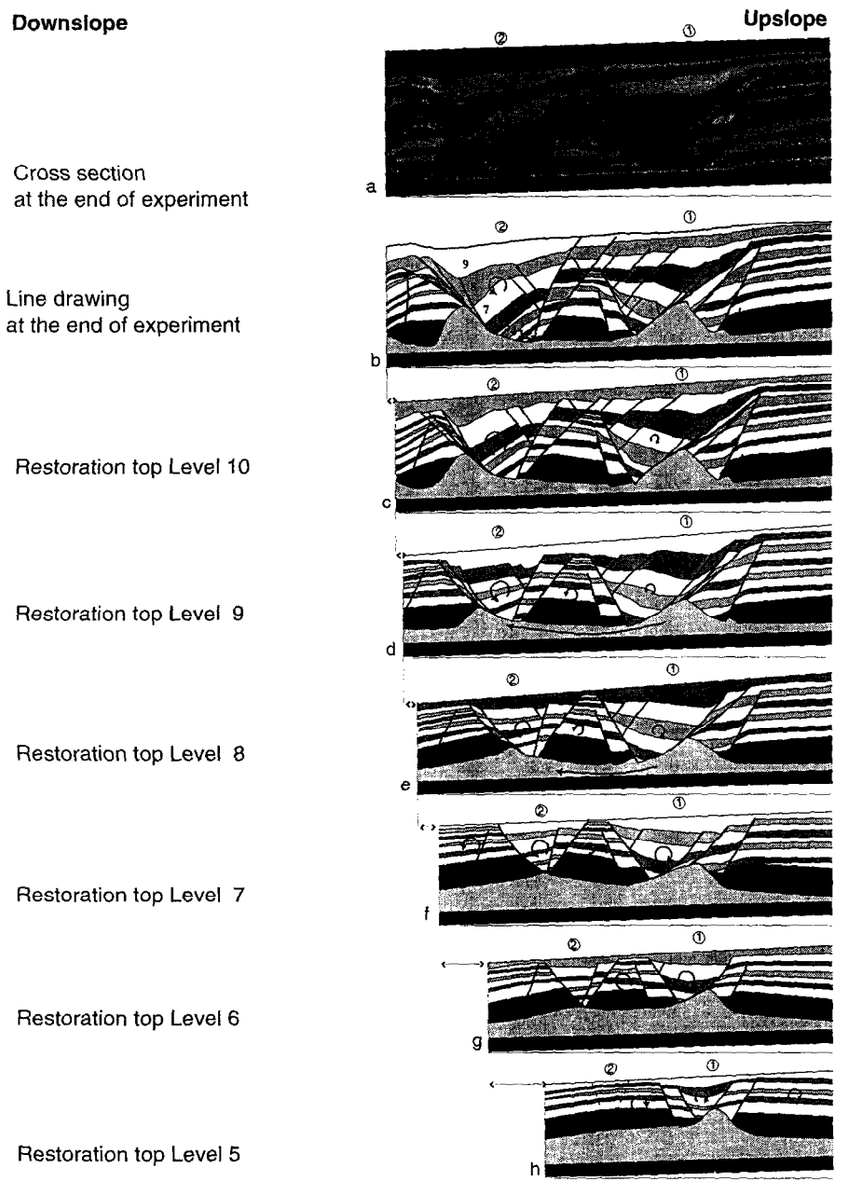

Figure 7 (a) Cross section of the turtle-back anticline obtained in the experiment shown in *Figure 6b–h* layer to layer palinspastic restoration

is the product of the viscosity and the shear strain rate, when the ductile layer thins, the strength increases (i.e. the coupling between sedimentary cover and basement increases). At constant strain rate, because the thickness of the ductile layer constantly decreases during gliding, the coupling constantly increases. From previous experiments where the structural effects of brittle-ductile coupling were analysed in detail (Allemand, 1990) we know that low coupling allows the development of symmetrical or nearly symmetrical structures and conversely that high coupling favours the development of asymmetrical ones (e.g. block tilting). For further details on the effect of brittle-ductile coupling on the development of listric growth fault, the reader could refer to Mauduit and Brun (1997). The observation of a transition from symmetrical to asymmetrical mode of deformation in both seismic lines and experiments is in agreement with this.

The role of diapirs

Our experiments (*Figures 4* and *5*) with palinspastic restorations, confirm that between-raft diapirs can play a significant role in the development of turtle-back anticlines [see also Vendeville and Jackson, (1992b) and Jackson *et al.* (1994)]. Our experiments show that the wrapping of rafts is achieved by a divergent rotation of synkinematic layers along diapirs limbs (*Figure 8a*).

Despite our efforts, we never succeed obtaining experimentally the so-called "Mock-turtle structures" (Vendeville and Jackson, 1992b): building of a turtle-back type depocentre which replaces a diapir between two rafts. Such structures were however observed on seismic sections (Duval *et al.*, 1992). It is interesting to note that, by opposition to raft wrapping (*Figure 4*), they would correspond to convergent rotations—by reference to the centre of the diapir—of synkinematic layers (*Figure 8b*).

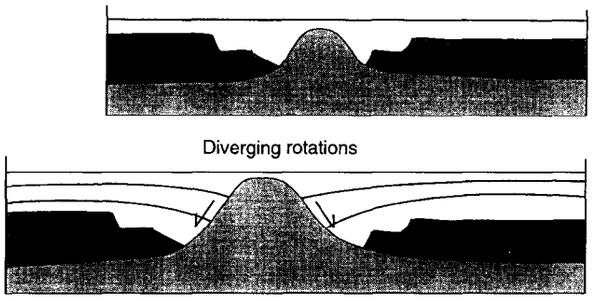

a Raft Wrapping

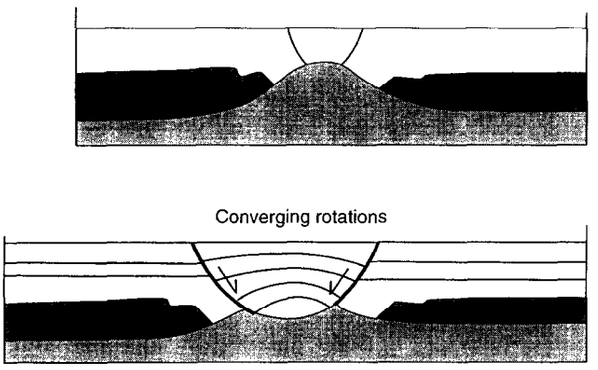

b Mock Turtle anticline

Figure 8 (a) Comparison of diapir fall induced layer rotations in the wrapping of rafts and (b) in the formation of a mock-turtle anticline

Whereas divergent rotations do not necessitate faulting (early stages on *Figure 5*) convergent rotations require two facing faults to work simultaneously (*Figure 8b*).

Transition in time from seaward to landward faulting

Both nature and experiments also provide evidences of turtle-back anticlines which develop in a purely asymmetric and/or diachronic way. In the examples quoted above, a seaward listric fault develops first, followed by a landward listric fault which can be partially synchronous (*Figures 6* and *7*) or entirely diachronous (*Figure 3*). Such turtle-back anticlines never passed through a symmetrical stage. Their asymmetry is initial. These examples also demonstrate that turtle-back anticlines do not necessarily need a diapir fall effect to initiate. An anticline can grow as soon as it is flanked by two facing listric growth faults working simultaneously or successively.

The transition in time from dominant seaward faulting to dominant landward faulting is also a consequence of brittle ductile coupling (as mentioned previously). Because the ductile layer thins faster upslope than downslope, coupling is stronger upslope than downslope. Consequently the seaward fault which is located on the upslope side of the anticline is slowed down and the landward fault which is located on the downslope side can move faster.

Acknowledgements

This work was financed by Elf Aquitaine. The models presented here are part of the MAD and MARGES projects (Modelisation Analogique des Deltas et Modelisation Analogique des Relations Entre la Gravité Et la Sédimentation) performed at Geosciences-Rennes and which aimed to study the interactions between sedimentation and faulting during the gravitational deformation. The authors acknowledge Geco-Prakla, Elf Angola and Elf Gabon for permission to use some seismic data and Elf Aquitaine to publish this paper. We thank J. J. Kermarrec for technical assistance in the Experimental Tectonics Laboratory, and M. Carpenter for improvement of the manuscript. Thanks are due to the referees M. P. A. Jackson and I. Davison who helped clarify several important points.

References

Brun, J. P. and Merle, O. (1985) Strain patterns in models of spreading-gliding nappes. *Tectonics* **4,** 705–719.

Cobbold, P. R. and Szatmari, P. (1991) Radial gravitational gliding on passive margins. *Tectonophysics* **188,** 249–289.

Cobbold, P. R., Szatmari, P., Demercian, L. S., Coelho, D. and Rosello, E. A. (1995) Seismic and experimental evidence for thin skin horizontal shortening by convergent radial gliding on evaporites, deep water Santos basin Brazil. In *Salt Tectonics: A Global Perspective*, eds M. P. A. Jackson, D. G. Robers and S. Snelson. *AAPG Mem.* **65,** 305–321.

Coward, M. and Stewart, S. (1995) Salt-influenced structure in the Mesozoic-Tertiary cover of the Southern North Sea U.K. In *Salt Tectonics: A Global Perspective*, eds M. P. A. Jackson, D. G. Roberts and S. Snelson. *AAPG Mem.* **65,** 229–250.

Demercian, S., Szatzmari, P. and Cobbold, P. R. (1993) Style and pattern of salt diapirs due to thin-skinned gravitational gliding, Campos and Santos basins. Offshore Brazil. *Tectonophysics* **228,** 393–433.

Diegel, F. A., Karlo, J. F., Schuster, D. C., Shoup, R. C. and R. Tauvers, P. (1995) Cenozoic structural evolution and tectonostratigraphic framework of the Northern Gulf Coast continental margin. In *Salt Tectonics: A Global Perspective*, eds M. P. A. Jackson, D. G. Roberts and S. Snelson. *AAPG MEm.* **65,** 109–151.

Duval, B., Cramez, C. and Jackson, M. P. A. (1992) Raft tectonics in the Kwanza (Cuenza) basin, Angola. *Mar. Petrol. Geol.* **9,** 389–404.

Heaton, R. C., Jackson, M. P. A., Bamahmoud, M. and Nani, A. S. O. (1995) Superposed Neogene extension, contraction and salt canopy emplacement in the Yemeni Red Sea. In *Salt Tectonics: A Global Perspective*, eds M. P. A. Jackson, D. G. Roberts and S. Snelson. *AAPG Mem.* **65,** 333–351.

Hooper, R. J. and More, C. (1995) Evaluation of some salt-related overburden structures in the U.K. Southern North Sea. In *Salt Tectonics: A global Perspective*, eds M. P. A. Jackson, D. G. Roberts and S. Snelson. *AAPG Mem.* **65,** 251–259.

Jackson, M. P. A., Vendeville, B. C. and Ela, D. D. S. (1994) Structural dynamics of salt systems. *Ann. Rev. Earth and Planet. Sci.* **22,** 93–117.

Liro, L. M. and Coen, R. (1995) Salt deformation history and postsalt structural trends, offshore Southern Gabon, West Africa. In *Salt Tectonics: A Global Perspective*, eds M. P. A. Jackson, D. G. Roberts and S. Snelson. *AAPG Mem.* **65,** 323–331.

Lundin, E. L. (1992) Thin skin extensional tectonics on a salt detachment, Northern Kwanza Basin, Angola. *Mar. Petrol. Geol.* **9,** 405–411.

Lundin, E. L. (1993a) A Geologic "tortoise and hare race" in the Northern Kwanza Basin, Angola. Gravity gliding vs gravity spreading. In *AAPG Int. Hedberg Res. Conf.*, Bath, England. Abstract.

Lundin, E. L. (1993b) The Northern Kwanza basin, Angola, an unusual example of raft tectonics on a salt layer. In *AAPG Int. Hedberg Res. Conf.*, Bath, England. Abstract.

Mauduit, T. and Brun, J. P. (1998) Growth fault/rollover systems: birth, growth and decay, *J. Geophys. Res.*, in press.

McClay, K. R. and Ellis, P. G. (1987) Analogue models of extensional fault geometries. In *Continental Extensional Tectonics*, eds M. P. Coward, J. P. Dewey and P. L. Hancock, vol. 28, pp. 109–125.

Merle, O. (1986) Patterns of stretch trajectories and strain rates

within spreading-gliding nappes. *Tectonophysics* **124,** 211–222.

Mohriak, W. U., Macedo, J. M., Castellani, R. T., Rangel, H. D., Barros, A. Z. N., Latgé, M. A., Ricci, J. A., Mizusaki, A. M., Szatmari, P., Demercian, L. S., Rizzo, J. G. and Aires, J. R. (1995) Salt tectonics and structural styles in the deep water province of the Cabo Frio Region, Rio de Janeiro, Brazil. In *Salt Tectonics: A Global Perspective*, eds M. P. A. Jackson, D. G. Roberts and S. Snelson. *AAPG Mem.* **65,** 305–321.

Nalpas, T. and Brun, J.-P. (1993) Salt flow and diapirism related to extension at crustal scale. *Tectonophysics* **228,** 349–362.

Peel, F. J., Travis, C. J. and Hossack, J. R. (1995) Genetic structural provinces and salt tectonics of the Cenozoic offshore U.S. Gulf of Mexico: a preliminary analysis. In *Salt tectonics: A Global Perspective*, eds M. P. A. Jackson, D. G. Roberts and S. Snelson. *AAPG Mem.* **65,** 153–175.

Remmelts, G. (1995) Fault related Salt Tectonics in the southern North Sea. The Netherlands. In *Salt Tectonics: A Global Perspective*, eds M. P. A. Jackson, D. G. Roberts and S. Snelson. *AAPG Mem.* **65,** 261–272.

Rowan, M. G. (1995) Structural styles and evolution of allochthonous salt, central Louisiana outer shelf and upper slope. In *Salt Tectonics: A Global Perspective*, eds M. P. A. Jackson, D. G. Roberts and S. Snelson. *AAPG Mem* **65,** 119–228.

Schuster, D. C. (1995) Deformation of allochthonous salt and evolution of related salt/structural systems, Eastern Louisiana Gulf Coast. In *Salt Tectonics: A Global Perspective*, eds M. P. A. Jackson, D. G. Roberts and S. Snelson. *AAPG. MEm.* **65,** 177–198.

Spathopoulos, F. (1996) An insight on salt tectonics in the Angola basin, South Atlantic. In *Salt Tectonics*, eds D. J. Blundel, G. I. Alsop and J. Davison. *Geol. Soc. Spec. Pub.* **100,** 153–174.

Stewart, S. A., Harvey, M. J., Otto, S. C. and Weston, P. J. (1996) Influence of salt on fault geometry: examples from the UK salt basins. In *Salt Tectonics*, eds D. J. Blundel, G. I. Alsop and J. Davison. *Geol. Soc. Spec. Pub.* **100,** 246–258.

Szatmari, P., Guerra, M. C. M. and Pequeno, M. A. (1996) Genesis of large counter regional fault by flow of Cretaceous salt in the South Atlantic Santos basin, Brazil. In *Salt Tectonics*, eds D. J. Blundel, G. I. Alsop and J. Davison. *Geol. Soc. Spec. Pub.* **100,** 259–264.

Teisserenc, P. and Villemin, J. (1989) Sedimentary Basin of Gabon. *In Geology and Oil Systems, Divergent/Passive Margin Basins*, eds J. D. Edwards and P. A. Santogrossi. *AAPG Mem.* **48,** 117–199.

Van Keken, P. E., Spiers, C. J., Berg, A. P. V. D. and Muyzert, E. J. (1993) The effective viscosity of rocksalt: implementation of steady state creep laws in numerical models of salt diapirism. *Tectonophysics* **225,** 457–476.

Vendeville, B. and Jackson, M. P. A. (1992a) The rise of diapirs during thin skinned extension. *Mar. Petrol. Geol.* **9,** 331–353.

Vendeville, B. and Jackson, M. P. A. (1992b) The fall of diapirs during thin skinned extension. *Mar. Petrol. Geol.* **9,** 354–371.

Worrall, D. M. and Snelson, S. (1989) Evolution of the Northern Gulf of Mexico with emphasis on Cenozoic growth faulting and the role of salt. In *The Geology of North America—An Overview*, eds A. W. Bally and A. R. Palmer. Boulder, CO, pp. 97–138.